Tebbe Paulsen, Nikolai Guba, Jens Sölter, Bernhard Karpuschewski

Influence of the workpiece material on the cutting performance in low frequency vibration assisted drilling

Journal Article as: peer-reviewed accepted version (Postprint)

DOI of this document*(secondary publication): https://doi.org/10.26092/elib/2424

Publication date of this document: 31/08/2023

* for better findability or for reliable citation

Recommended Citation (primary publication/Version of Record) incl. DOI:

Tebbe Paulsen, Nikolai Guba, Jens Sölter, Bernhard Karpuschewski,
Influence of the workpiece material on the cutting performance in low frequency vibration assisted drilling,
CIRP Journal of Manufacturing Science and Technology,
Volume 31, 2020, Pages 140-152, ISSN 1755-5817,
https://doi.org/10.1016/j.cirpj.2020.10.003

Influence of the workpiece material on the cutting performance in low frequency vibration assisted drilling

Tebbe Paulsen[a,b,*], Nikolai Guba[a,b], Jens Sölter[a,b], Bernhard Karpuschewski[a,b]

[a] Leibniz Institute for Materials Engineering, Division Manufacturing Technologies, Badgasteiner Straße 3, 28359 Bremen, Germany
[b] University of Bremen and MAPEX Center for Materials and Processes, Bibliothekstr. 1, 28359 Bremen, Germany

Keywords:
Vibration drilling
Chip deformation
Workpiece material

A B S T R A C T

Fundamental problems in drilling processes are associated with the unfavorable machining conditions in the tool center and the difficult chip removal. Low frequency vibration assisted drilling (LFVAD), in which the linear tool feed is superimposed with a vibratory motion in feed direction, is a promising process to overcome these problems. Aiming at a systematic analysis of the influence of workpiece material properties, results from LFVAD experiments with Ti6Al4V, AlMgSi0.5 and 42CrMo4 in different heat treatment states are presented. Specifically the dependence of optimal oscillation amplitudes on the workpiece material behavior is analyzed.

Introduction

Due to the unfavorable machining conditions and the difficult chip removal in drilling processes, vibration assistance is increasingly used to overcome these problems. The main focus of the present paper is the influence of the workpiece material on the cutting performance in vibration assisted drilling processes with high amplitudes and small frequencies. In low frequency vibration assisted drilling processes (LFVAD) the continuous, axial feed movement of the tool is superimposed by a sinusoidal oscillation with an amplitude, high enough to compensate the feed movement of the tool for short time periods, leading to an interrupted cut and a kinematically enforced chip breakage. The generation of oscillations in feed direction can be realized with mechanical systems, with piezo or hydraulic actuators [1] or, like in the present work, with a spindle with magnetic bearings, allowing a CNC-controllable adjustment of the amplitude A and specific frequency Fs, independently of the spindle speed [2,3]. A characteristic attribute of this process is the interrupted cut, which leads to small chips and an increased chip removal quality [4]. Furthermore, the process temperature can be reduced significantly, which can be explained by the reduced chip friction, better cooling and lubrication of the borehole ground and the interrupted cut, leading to short cool-down times during the process [5]. As a result, negative impacts on the subsurface properties of metallic workpieces can be avoided [6] and the formation of an exit burr, which can have a significant influence on the fatigue performance [7], can be reduced [4]. Due to these advantages, low frequency vibration assisted drilling is widely used in the aircraft industry, especially for machining processes of hard to cut materials or CFRP/metal-compounds. In drilling processes of CFRP/metal-compounds with workpiece materials like titanium or aluminium alloys, the tendency to build long helical chips results in chip friction and damages in the sensitive CFRP layer. A reproducible and stable generation of small chip segments can help to avoid these problems [2,8,9]. Fig. 1 shows the engagement conditions in this process. The X-axis shows one full tool rotation (360°) and the Y-axis shows the actual position of the two cutting edges of a double-edged drilling tool (green and blue). Therefore, the two cutting edges are shifted by 180 degree. Furthermore, the calculated, uncut chip geometry can be identified, including the uncut chip radian α_{cu}, the maximum uncut chip thickness h_{max} and the borehole ground surface, generated in the previous tool rotation [10].

State of the art in LFVAD

A further development of this kinematic model, shown in Fig. 1, has been created in Matlab. This version enables an automated calculation of the uncut chip geometry for each possible parameter combination of feed per revolution f, amplitude of the oscillation A and specific oscillation frequency per revolution F_s. Changes of the spindle speed (cutting speed v_c) do not influence the uncut chip geometry.

* Corresponding author at: Leibniz Institute for Materials Engineering, Division Manufacturing Technologies, Badgasteiner Straße 3, 28359 Bremen, Germany.
E-mail address: paulsen@iwt-bremen.de (T. Paulsen).

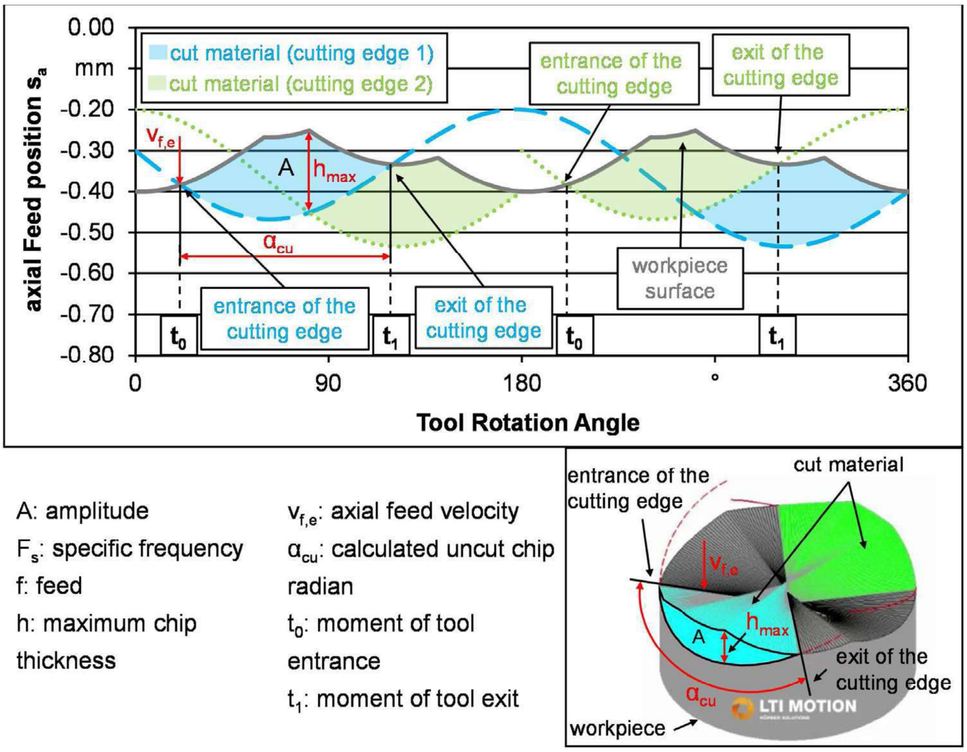

Fig. 1. Engagement conditions in low frequency vibration assisted drilling according to Ref. [10] (For interpretation of the references to colour in the text, the reader is referred to the web version of this article).

An important parameter for the characterization of LFVAD in the kinematic Matlab-model, is the calculated percentual cutting time $p_{cut,u}$. The percentual cutting time is a result of the combination of the feed f, the amplitude A and the specific frequency F_s and has been introduced in this model to enable amplitude recommendations with one single value. With this value for $p_{cut,u}$ it is possible to determine the optimal amplitude for each possible feed f. $p_{cut,u}$ represents the percentage of one complete tool oscillation in which the main cutting edges are in contact with the workpiece or rather the time, in which the two chips are generated (Δt_{cut}, from t_0 to t_1 in Fig. 1). The rest of the time (interrupted cutting time Δt_{inter}), the tool is not in contact with the workpiece and the generated chips are removed.

Increasing feed rates f at the same amplitude A are leading to higher percentual cutting times $p_{cut,u}$ in which the tool is in contact with the workpiece. As a consequence, the values for the (uncut) chip radian α_c (α_{cu}) are increasing, too. In order to keep the same uncut chip radian α_{cu} and ensure a consistent chip removal quality with an increasing feed f, it is necessary to increase the amplitude of the oscillation A. Therefore, it is possible to define a reliable process for different feeds f, if the one workpiece material dependent percentual cutting time $p_{cut,u}$ is known. With reliable information about $p_{cut,u}$, it is possible to calculate matching amplitudes A for each possible feed f and generate parameter tables for LFVAD applications.

The kinematic model mentioned above enables a calculation of the required amplitude for different feeds f at a consistent, predefined percentual cutting time $p_{cut,u}$. Compared to conventional drilling the uncut chip thickness varies in LFVAD, resulting in varying feed forces and cutting torques. Details regarding the prediction of the resulting maximum feed forces and feed force evolution over single tool engagements can be found in Ref. [11].

For reliable LFVAD of different materials, reasonable values for the cutting speed v_c, the feed per revolution f, the oscillation frequency per revolution F_s and the amplitude A have to be chosen. Appropriate values for the cutting speed and feed are already well known for conventional drilling. The influences of different specific frequencies per revolution F_s in vibration assisted drilling have been investigated extensively in Refs. [10,12]. Regarding usable ranges of amplitudes, initial indications for Ti6Al4V can be found in Refs. [9,10,12]. Nevertheless, for an optimal amplitude selection, no conclusions can be found in literature, taking into account different workpiece material properties and feeds. Therefore it is not possible to provide recommendations concerning the amplitude A or more specifically, the optimal percentual cutting time $p_{cut,u}$ for different materials.

Target of research and procedure

The target of research was to gain more insight regarding the chip formation in LFVAD, particularly the influence of the workpiece material properties.

A second target was to identify one specific value for each workpiece material, characterizing a reasonable selection of the oscillation amplitude A in LFVAD processes for different feeds f. Therefore, the percentual cutting time $p_{cut,u}$ has been introduced, which is dependent on the feed per revolution f and the oscillation amplitude A at a fixed specific frequency. The percentual cutting time $p_{cut,u}$ is a direct equivalent to the uncut chip radian α_{cu}. Therefore, it is possible to define one value for each material, characterizing a related amplitude A for each possible feed rate f. With this information, a linear relationship between desired feed rate f and needed optimal amplitude A can be presented. Due to the wide range of material properties, investigated in this paper, and the related correlations, these investigations can help to choose optimal percentual cutting times, even for other workpiece materials with similar properties. Fig. 2 shows the schematic procedure of the planned investigations.

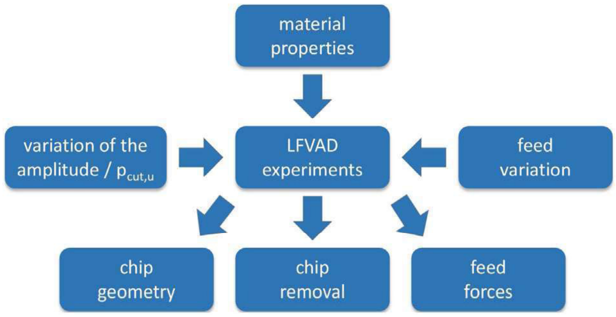

Fig. 2. Schematic procedure.

To provide conclusive results, the following range of workpiece materials (Table 1) with different material properties has been chosen for the investigations.

It has to be mentioned, that the aluminium alloy shows a low ductility at a low elongation at break with a comparatively high strength, due to its heat treatment. However, compared to the other investigated workpiece materials, the strength is very low. The steel alloy 42CrMo4 has been investigated in three different heat treatment conditions from low strength/hardness values at high ductility (199 HV) to high strength/hardness at a low ductility (499 HV). Preliminary considerations and investigations led to the assumption, that the strength has a significant influence on the chip compression in the process and therefore, on the resulting chip size and chip removal. Considerations on the dissolution of the chip from the main cutting edge led to the assumption, that the adhesion tendency has a big influence on the time the chip needs to dissolve and be removed out of the cutting zone. Therefore, workpiece materials with differing adhesion tendencies have been chosen [13,14]. Furthermore, the widely differing elastic modulus of the materials can have an influence on elastic deformations of the generated borehole ground, which can affect the chip geometry and chip removal as well. Due to the interrupted cut, the chip breakage, and in this context the toughness and ductility, was assumed to be secondary for the chip generation and chip removal.

Experimental setup and methods

In pretrials a range of five percentual cutting times $p_{cut,u}$ in steps of 2.5 % have been defined for each workpiece material, ensuring chip breakage. These five percentual cutting times $p_{cut,u}$ have been applied to five different feed rates from f = 0.05 mm/rev. to f =0.15 mm/rev. With a rising feed rate f, the amplitude A has to be increased, to achieve the same percentual cutting time $p_{cut,u}$. Therefore, each combination of feed rate f and percentual cutting time $p_{cut,u}$ results in a specific amplitude A. The experimental plan, which has been processed full factorial, can be seen in Table 2.

For the investigations, a cutting speed of v_c = 15 m/min and v_c = 60 m/min has been applied and a specific frequency of F_s = 1.5 osc./rev. has been used, based on findings in Refs. [4,10,12]. Each drilling trial has been repeated three times. For the drilling investigations, solid tungsten carbide tools (twisted, two cutting edges), have been used (see Fig. 3). The tools were uncoated, when drilling AlMgSi0.5 and Ti6Al4V and coated (TiAlSiN), when drilling 42CrMo4. As internal MQL, fatty alcohol at a pressure of p_{MQL} = 7.5 bar has been used. Due to the high strength values of Ti6Al4V and 42CrMo4 – 499 HV, the feed f has not been increased above 0.1 mm/rev for these materials.

Fig. 4 shows the resulting amplitude for each combination of feed f and percentual cutting time $p_{cut,u}$. Parameter combinations which result in amplitudes above A = 150 µm are missing due to physical limits of the used magnetic spindle.

Fig. 5 shows an overview of the evaluated processes (vibration assisted drilling and conventional drilling; the latter being characterized by a percentual cutting time of $p_{cut,u}$ = 100 %).

Additionally it shows the evaluation criteria, which are explained in detail below.

Chip geometry

During chip formation, a compression and plastic deformation of the chip takes place, leading to decreased values of the chip radian α_c compared to the uncut chip radian α_{cu}. Therefore, the chip radians α_c have been determined by measuring the arc length in the top view under a microscope. This was necessary, due to differently developed curvatures of the chips, limiting an exact measurement in the side view which can be seen in the results. Furthermore, it has been determined if process reliable chip breakage took place and if the chips are separated from each other and no welded and strongly deformed chips have been generated, due to friction and chip accumulation. These indications of process disturbances have been considered as one criterion for the selection of optimal percentual cutting times.

Chip removal quality

The chip removal quality can be quantified by the evaluation of the chip removal index c_r and has been determined by high-speed

Table 1
Investigated workpiece materials and relevant properties.

Workpiece material	Strength/tensile strength Rm [N/mm^2]	Ductility/elongation at break [%]	Adhesion tendency	Elastic modulus [GPa]
Ti6Al4V	High/1030	High/16	High	114
AlMgSi0.5	Very low/215	Very low/8	Very high	70
42CrMo4 199 HV	Low/733	Very high/28	Low	210
42CrMo4 333 HV	High/1050	High/16	Low	
42CrMo4 499 HV	Very high/1567	Very low/8	Low	

Table 2
Experimental design.

Workpiece material	Feed f [mm/rev]	Percentual cutting time $p_{cut,u}$ [%]
Ti6Al4V	0.05, 0.075, 0.1	47.5, 45, 42.5, 40, 37.5
AlMgSi0.5	0.05, 0.075, 0.1, 0.125, 0.15	62.5, 60, 57.5, 55, 52.5
42CrMo4, 199 HV	0.05, 0.075, 0.1, 0.125, 0.15	65, 62.5, 60, 57.5, 55
42CrMo4, 333 HV	0.05, 0.075, 0.1, 0.125	62.5, 60, 57.5, 55, 52.5
42CrMo4, 499 HV	0.05, 0.075, 0.1	55, 52.5, 50, 47.5, 45

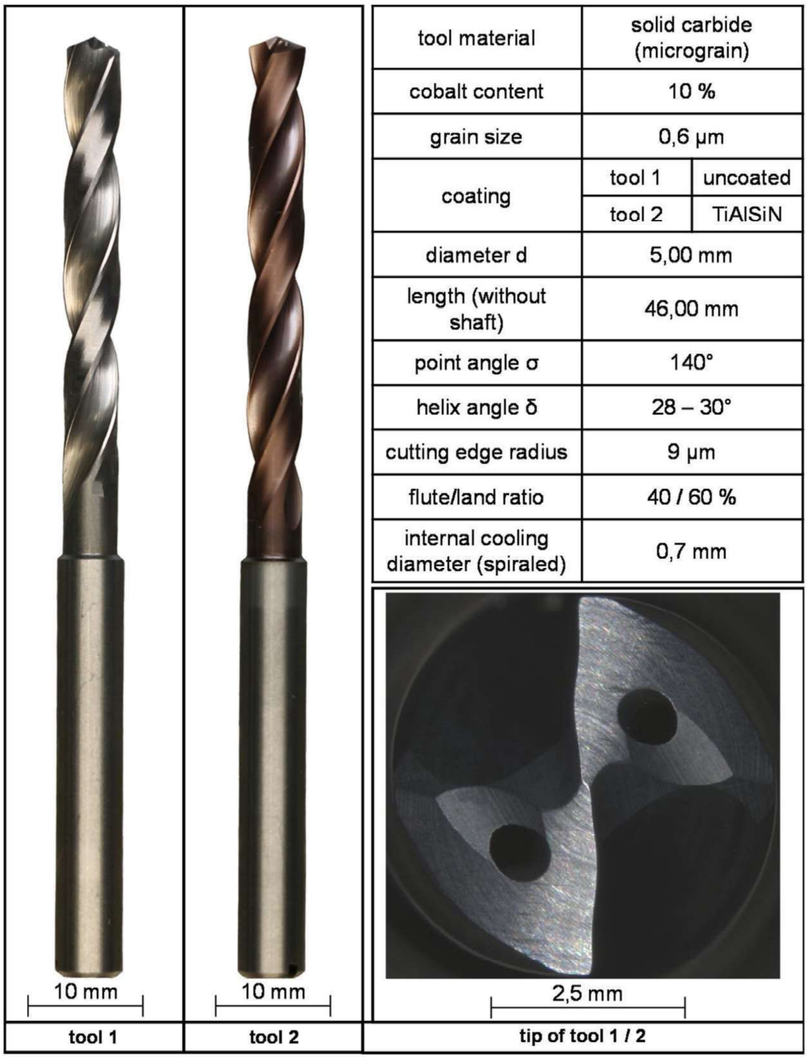

tool material	solid carbide (micrograin)	
cobalt content	10 %	
grain size	0,6 µm	
coating	tool 1	uncoated
	tool 2	TiAlSiN
diameter d	5,00 mm	
length (without shaft)	46,00 mm	
point angle σ	140°	
helix angle δ	28 – 30°	
cutting edge radius	9 µm	
flute/land ratio	40 / 60 %	
internal cooling diameter (spiraled)	0,7 mm	

Fig. 3. Cutting tools, used for the investigations.

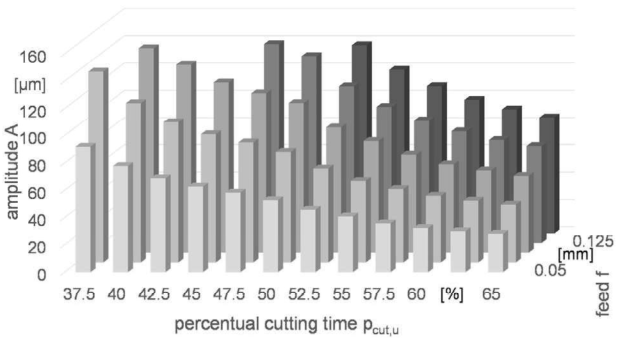

Fig. 4. Resulting amplitude A for all investigated combinations of feed f and percentual cutting time $p_{cut,u}$.

videos, recorded with a high-speed camera (1000 fps). An exemplary section of a high-speed-video can be seen in Fig. 6. Each tool-workpiece contact generates two chips. Therefore, the chip formation frequency f_{th} is known and dependent on the process parameters. By the observation of the chip extraction with a high-speed camera, the chip removal frequency f_m can be determined [4]. For an unhindered chip removal, the chip removal frequency would be the same as the chip formation frequency and the chip removal index c_r would be equal to 1 (according to Eq. (1) below). $\widehat{c}_V$ represents the empirical variation coefficient, calculated by the ratio between the standard deviation s and the root mean square RMS.

$$c_r = \frac{f_m}{f_{th}} * (1 - \widehat{c}_V) \ \ with \ \ \widehat{c}_V = \frac{\sigma(f_m)}{RMS(f_m)} \tag{1}$$

With an increasing difference between chip formation frequency f_{th} and chip removal frequency f_m, the chip removal quality decreases. A more detailed explanation of this approach to quantify the chip removal quality can be found in Ref. [4].

For all relevant drilling processes, the chip removal index has been evaluated by means of the generated high-speed videos. In experimental drilling processes, it is not possible to reach ideal conditions without any friction and chip adhesion. For this reason, a minimum value of $c_r = 0.6$ has been defined as a minimum chip removal quality for the selection of optimal percentual cutting times.

Amplitude deviation

The internal high-precision position sensor in the magnetic spindle enables a full monitoring of the internal rotor of the spindle. Therefore, the generated oscillation and amplitude has been monitored for all experiments. This has been used to ensure

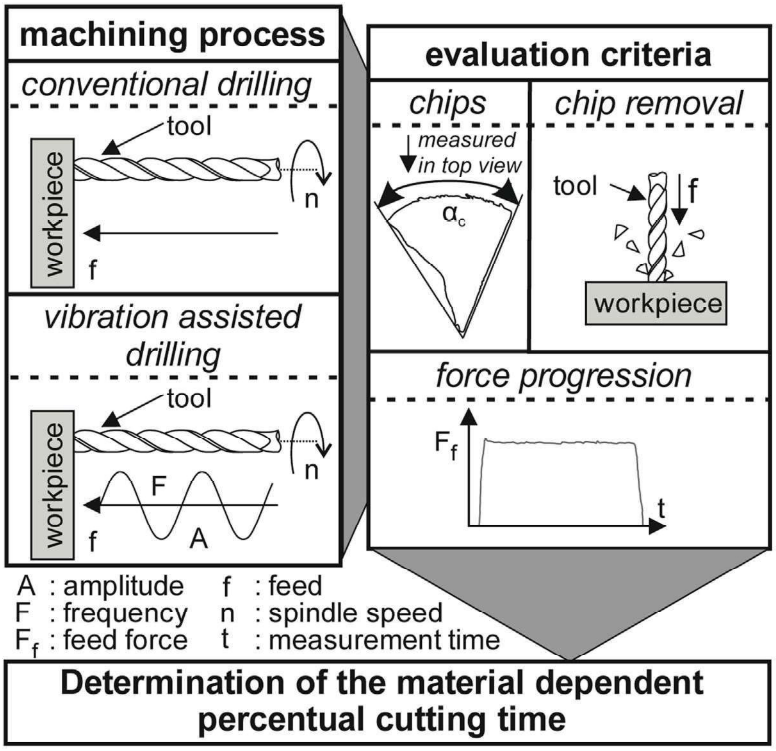

Fig. 5. Evaluated processes and evaluation criteria.

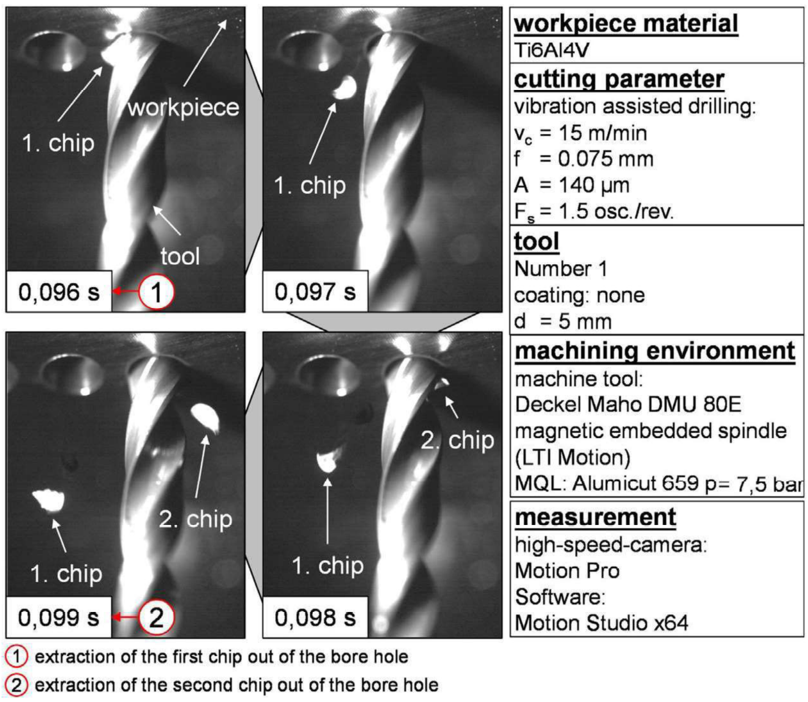

Fig. 6. Exemplary section of a high-speed-video.

that the desired amplitude was reached in all processes and that no process disturbances changed the desired sine curve.

Feed force measurement

Using a Kistler 3-component dynamometer at a measurement frequency of 4000 Hz, feed force measurement plots have been generated. These force measurement plots have been used to determine the maximum feed force, to control if the used amplitude has been high enough to ensure an interrupted cut (feed force decreases to 0 N for each oscillation) and to determine chip accumulation. In the case of chip accumulation along the drill flutes, maximum forces increase and minimum forces do not vanish at tool lift-off. Therefore, a constant maximum feed force over the whole drilling process is desired. Additionally, the individual cutting times $t_{cut,i}$ and the interrupted cutting times $t_{inter,i}$ have to stay at constant values, which has been an additional criterion for the selection of optimal percentual cutting times.

Experimental setup

Fig. 7 shows the experimental setup, which enables an investigation of the previously explained evaluation criteria. It shows the magnetic embedded spindle, used to generate the superimposed oscillation, the high-speed camera, used to monitor the chip removal, and the workpiece attachment, ensuring a stiff clamping on the 3-component dynamometer.

Results and discussion

Chip geometry

In order to evaluate the chip removal quality and the chip formation, the chip geometry has been investigated as a first step. Fig. 8 shows an exemplary selection of chip geometries of AlMgSi0.5, 42CrMo4–499 HV and Ti6Al4V. The figure shows different chip geometries for different feeds per revolution f (rows) and percentual cutting times $p_{cut,u}$ (columns). Red and green frames indicate, if the chip is acceptable or if there are any indications for an unfavorable chip formation (strong plastic deformation, connected/welded chips and signs of chip accumulation, respectively). Obviously, the chip radians α_c decreased with a decreasing percentual cutting time $p_{cut,u}$ (increasing amplitude A at a constant oscillation frequency). For AlMgSi0.5, desirable chip geometries are generated at a percentual cutting time of $p_{cut,u}$ = 52.5%. Due to the higher strength, the percentual cutting time has to be significantly lower for 42CrMo4–499 HV (45%). For Ti6Al4V a percentual cutting time of $p_{cut,u}$ = 42.5%, resulting in a significantly increased amplitude, is necessary. A low feed value of f = 0.5 mm and a high oscillation amplitude of A = 92 μm (percentual cutting time $p_{cut,u}$ = 37.5%) revealed an unfavorable chip geometry as well. This phenomenon is connected to the minimum chip thickness and the short cutting times in this process. Due to the low feed rate, material ploughing increases as the uncut chip thickness decreases. Especially the frequent new start of the cut causes problems, because the minimum chip thickness has to be exceeded for each new cut. The influence of this effect possibly increases, when cutting tools with a bigger cutting edge radius are used.

Resulting optimal amplitude

Based on the measurement data and presented criteria, an optimal percentual cutting time $p_{cut,u}$ has been defined for all workpiece materials. With this information, the optimal amplitude for each possible feed can be determined, using the linear relationship between feed f and amplitude A at a fix percentual cutting time (see Fig. 9).

The measurement data, used to determine these optimal values, was consisting of the presented criteria:

- Favorable chip geometry: no indications of strong plastic deformation as a sign of chip friction and chip accumulation
- Chip removal index: minimum 0.6
- Force measurement: process reliable interruption of the cut, even level of the maximum feed force over the whole drilling process and no other indications for chip friction/process disturbances

The following Fig. 9 shows the percentual cutting times $p_{cut,u}$, defined on the basis of the presented criteria. The results show significant differences between the optimal amplitudes when drilling different workpiece materials and can be used to define process designs for desired LFVAD processes in different workpiece materials. It can be seen, that a low optimal percentual cutting time

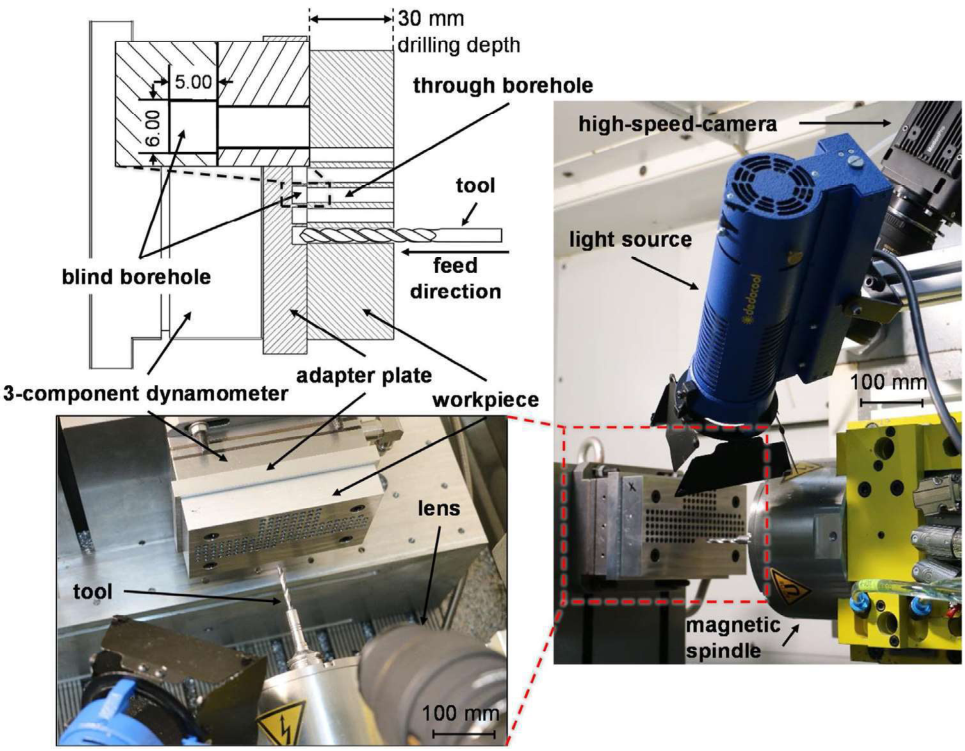

Fig. 7. Experimental setup.

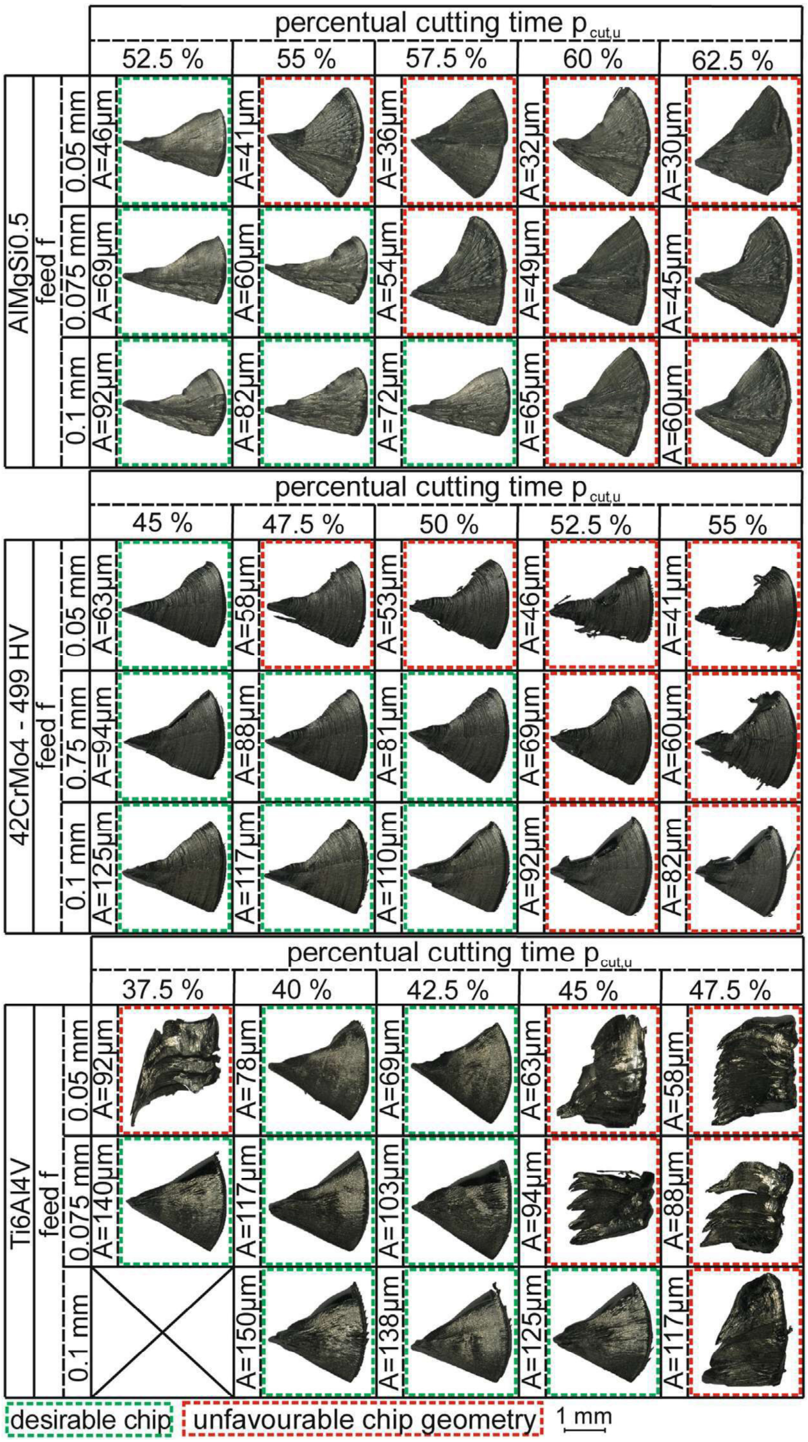

Fig. 8. Exemplary chip geometries of AlMgSi0.5, 42CrMo4 and Ti6Al4V (For interpretation of the references to colour in the text, the reader is referred to the web version of this article).

results in a higher slope of the graph, leading to a significant increase of the needed optimal amplitude for increased feed rates. Furthermore, it can be noted, that the recommended amplitude for AlMgSi0.5 and 42CrMo4−333 HV is the same, although the resulting chip radians differ from each other significantly. This circumstance is related to the different tendency to adhesions of these materials and is explained in more detail in Section “Influence of the workpiece material on the chip geometry and chip removal quality”.

Influence of the workpiece material on the chip geometry and chip removal quality

A comparison between the chip radian α_c and the calculated, uncut chip radian α_{cu} reveals a workpiece material-specific difference. Due to chip compression, the resulting chip radian α_c decreases. When drilling 42CrMo4 at different heat treatment conditions, the influence of the increasing hardness (strength) values becomes obvious.

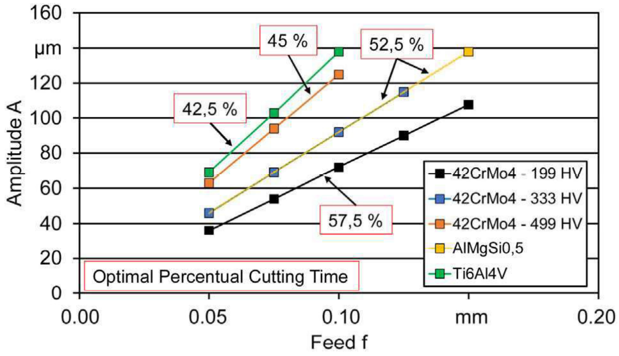

Fig. 9. Resulting optimal amplitudes A for different feed values f and workpiece materials.

Fig. 10 shows exemplarily the deviation between the uncut chip radian α_{cu} and the resulting chip radian α_c after drilling investigations at a feed of f = 0.1 mm and all investigated percentual cutting times $p_{cut,u}$, including the optimal value determined in Section "Resulting optimal amplitude".

With a decreasing percentual cutting time $p_{cut,u}$ (increasing amplitude A) α_c and α_{cu} decrease. The figure is showing that the calculated linear chip radian progression for increasing percentual cutting times can be seen in the resulting radian of the measured chip as well. The progression of both values constitute parallels, characterizing the material-specific chip compression. Increasing hardness (strength) values lead to a lower chip compression and, as a result, to higher chip radians α_c.

Therefore, the percentual cutting time $p_{cut,u}$ has to be lower for materials with high hardness (strength) values, in order to generate chips, small enough for a reliable chip removal. Noticeable are the resulting chip radians α_c of the selected optimal amplitude when drilling 42CrMo4. For each heat treatment condition, the resulting chip radian α_c of the optimal amplitude has been approximately $\alpha_c = 70°$.

In contrast, the results when drilling Ti6Al4V and AlMgSi0.5 show significant deviations regarding the optimal percentual cutting time $p_{cut,u}$ and the resulting chip radians α_c (see Fig. 11).

The resulting chip radians of Ti6Al4V show significantly higher values with a chip radian at the selected optimal parameter of $\alpha_c = 90°$, although the investigated percentual cutting times $p_{cut,u}$ were lower. Due to the strength of the material, even at high process temperatures, the chip compression is very low, leading to bigger resulting chips. Additionally, Ti6Al4V has an adhesion tendency. Therefore, the chips need a longer interrupted cutting time $t_{inter,i}$ to lift-off from the cutting edge. Otherwise, the chip still sticks at the tool when the main cutting edges are entering the material the next time, which results in chip accumulation. Additionally, the low chip compression itself leads to bigger chips, which need more time to be transported away from the cutting zone within the restricted chip space of the tool.

Regarding the chip radians α_c of AlMgSi0.5, it is obvious that the chip compression is very strong, resulting in very small chips. Nevertheless a percentual cutting time of $p_{cut,u}$ = 52.5 % is needed to achieve a sufficient chip removal quality. This shows impressively, that the generation of small chips does not necessarily lead to a sufficient chip removal quality. Due to the high adhesion tendency, increased interrupted cutting times $t_{inter,i}$ are needed to lift-off the chips from the cutting edges and to transport them away from the cutting zone.

The influence of the workpiece material on the resulting chip geometry and the amplitude, needed for a sufficient chip removal, can be summarized as follows. Workpiece materials with high hardness and strength values show low chip compression, resulting in bigger chips. Therefore, the percentual cutting time has to be decreased to generate chips which are small enough to be extracted without any disturbances. For workpiece materials with low hardness and strength values but with a strong tendency to

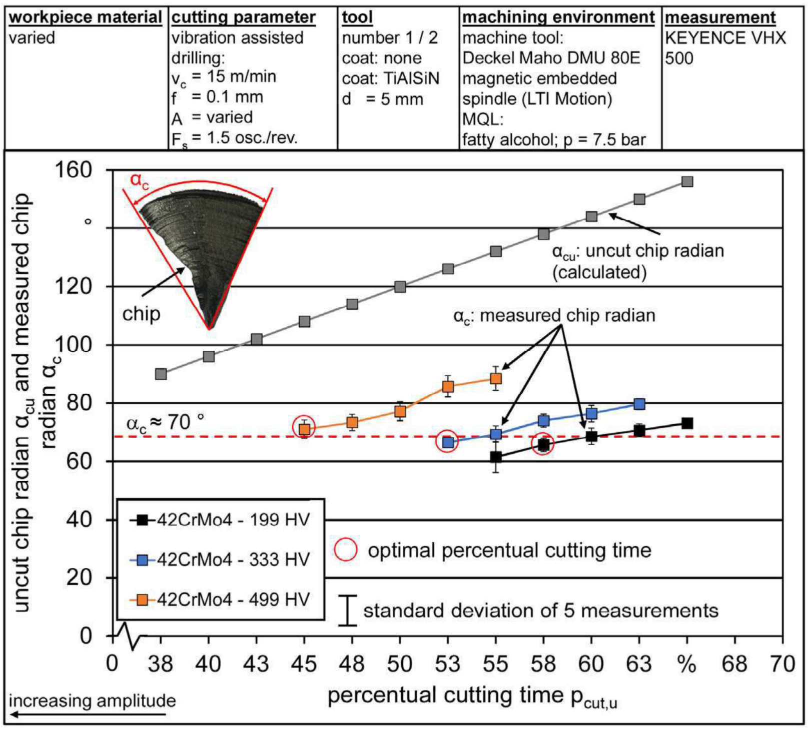

Fig. 10. Uncut chip radian α_{cu} and chip radian α_c after drilling of 42CrMo4 in different heat treatment conditions at a feed of f = 0.1 mm in dependence of the percentual cutting time $p_{cut,u}$.

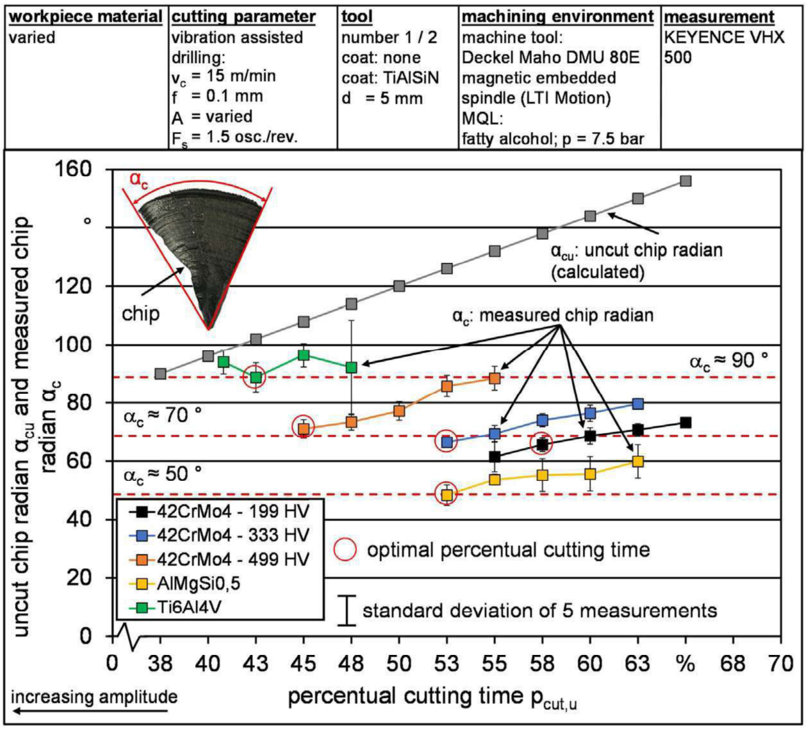

Fig. 11. Uncut chip radian α_{cu} and chip radian α_c after drilling of 42CrMo4 in different heat treatment conditions, AlMgSi0.5 and Ti6Al4V at a feed of f = 0.1 mm in dependence of the percentual cutting time $p_{cut,u}$.

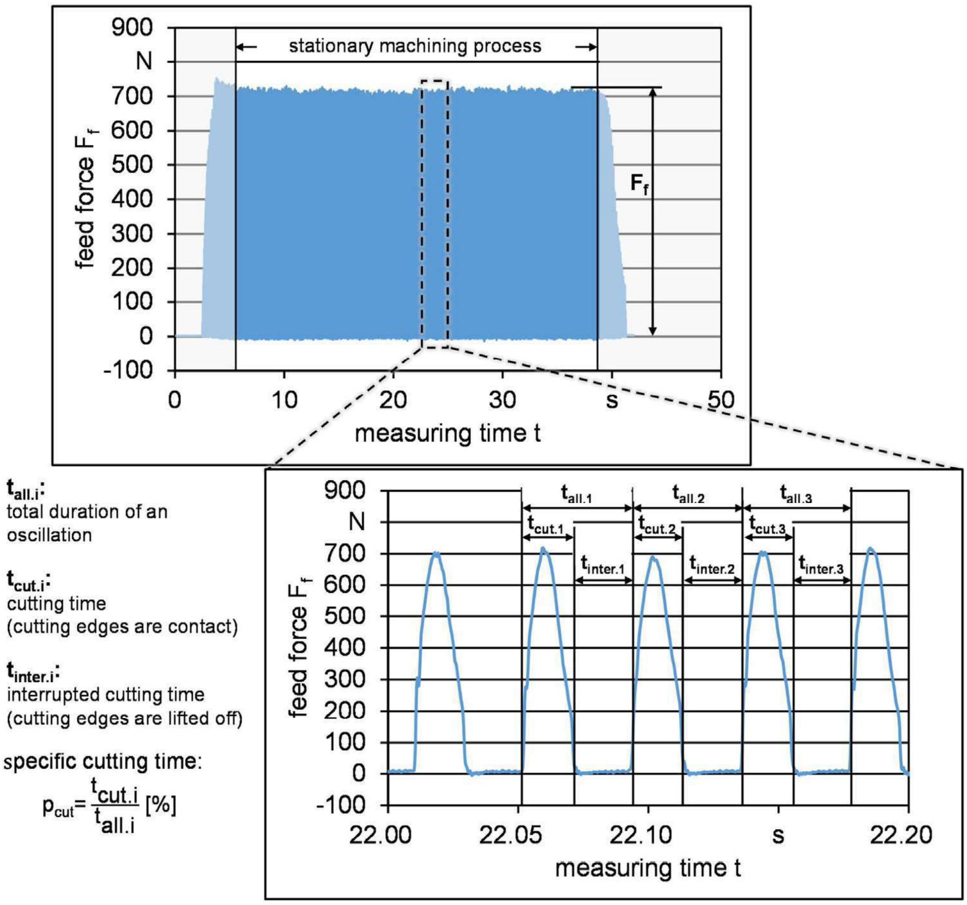

Fig. 12. Force measurement plot of a LFVAD process.

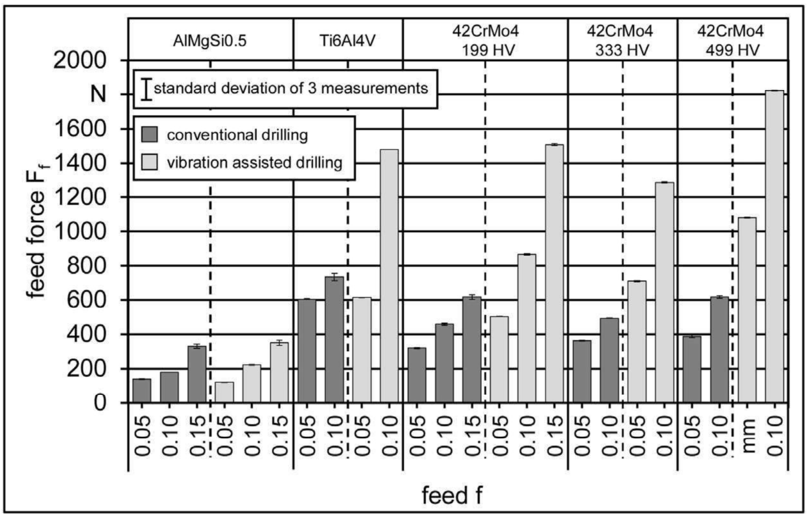

Fig. 13. Maximum feed force of LFVAD and conventional drilling.

adhesions, the resulting chips in reliable processes are significantly smaller than necessary. The important factor in this case is the adhesion tendency. To ensure a reliable chip removal, the interrupted cutting time has to be high enough to ensure enough time for the chip to be transported away from the chip formation zone. As a result, the recommended percentual cutting time for AlMgSi0.5 and 42CrMo4–333 HV is the same, although the chip radians of AlMgSi0.5 are significantly smaller. At a combination of high (temperature) strength values and an adhesion tendency, very low percentual cutting times are required (see Ti6Al4V). Due to the comparatively low elastic modulus of Ti6Al4V in combination with the high feed forces, elastic deformation of the generated borehole ground is presumed, leading to longer contact times and higher chip radians. The low elastic modulus of AlMgSi0,5 has a comparatively low impact on the chip sizes, due to the very low feed forces in the machining process. The ductility or toughness of the workpiece material seems to be less relevant, due to the interrupted cut in LFVAD, leading to an enforced chip breakage.

A reasonable basis for the oscillation amplitude selection can be taken from Fig. 9, when drilling workpiece materials with similar material properties. At this point it is important to mention, that the optimal amplitude can be dependent on other boundary conditions like the tool geometry (chip space, cutting edge radius and the size of the internal coolant holes), the stiffness of the workpiece clamping and the MQL pressure/flow rate, as well. Therefore, it is possible that these values have to be slightly adjusted, for example when using tools with an exceptionally small chip space, higher values for the cutting edge radius or a workpiece clamping with a low stiffness.

Resulting feed forces

In LFVAD processes without any disturbances, the maximum feed force is constant without any variation (see Fig. 12). In contrast to this, conventional drilling of materials, leading to long chips, results in chip accumulation and high friction, leading to an increasing feed force over the drilling cycle and a high thermomechanical load for tool and workpiece.

In Fig. 13 the maximum feed forces for LFVAD and conventional drilling processes are exemplary shown. Increased feed forces due to chip accumulation at increased drilling depths for conventional drilling have not been taken into account.

LFVAD results in significantly higher maximum uncut chip thicknesses h_{max} compared to the constant uncut chip thickness in conventional drilling. The influence of this effect increases with increasing oscillation amplitudes. For both drilling processes, the resulting feed forces are strongly dependent on the workpiece material strength. In LFVAD of materials with high strength values, for which higher amplitudes are applied, lead to an additional increase of the feed force. Similarly, if the feed in LFVAD is increased, the optimal oscillation amplitude has to be increased too, in order to reach optimal percentual cutting times. This leads to higher maximum uncut chip thicknesses during the process. As a result the difference of the maximum feed force between conventional drilling and LFVAD increases with increasing axial feed.

Influence of increased cutting speeds

When drilling AlMgSi0.5 and 42CrMo4, usually higher cutting speeds than 15 m/min are used. Therefore, the influence of a

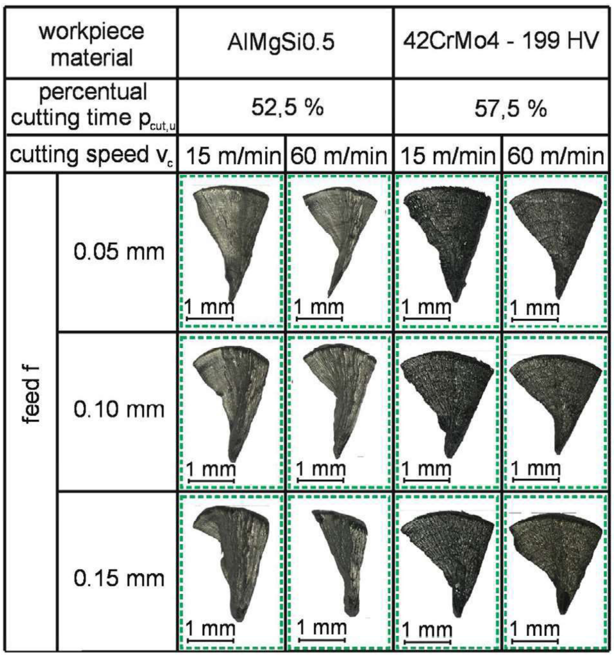

Fig. 14. Comparison of chips, resulting from drilling processes at different cutting speeds (AlMgSi0.5 and 42CrMo4–199 HV).

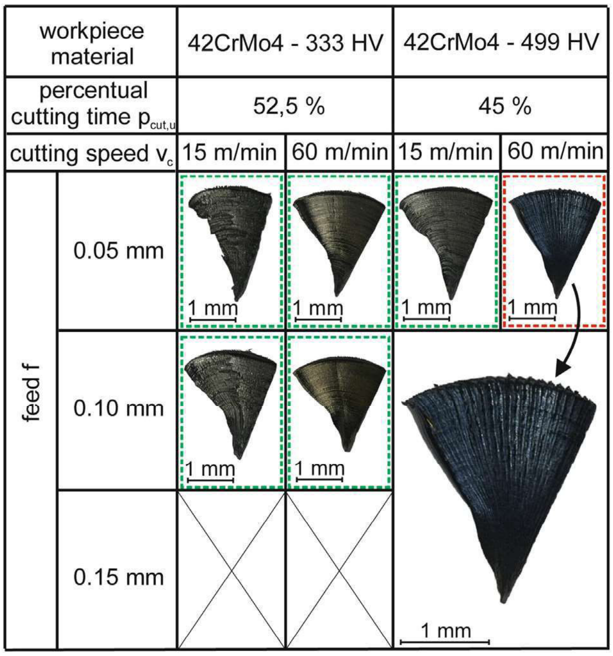

Fig. 15. Comparison of chips, resulting from drilling processes at different cutting speeds (42CrMo4–333 HV and 42CrMo4–499 HV).

cutting speed of v_c =60 m/min on the key findings presented before has been investigated and compared. Apart from the cutting speed all process parameters have been held constant.

Figs. 14 and 15 are showing a comparison between the chips resulting from drilling processes with 15 m/min and 60 m/min.

When drilling 42CrMo4 at v_c = 60 m/min (Fig. 15, on the right), a strong noise emission and visible chatter marks on the resulting chips occurred, which probably can be attributed to torsional stresses in the tool. Furthermore, annealing colors could be observed for 42CrMo4, indicating expectable higher process temperatures for higher cutting speeds.

The measurement of the chip radians α_{cu} revealed slightly higher values, resulting from processes with higher cutting speeds (see Fig. 16).

The increased values of the chip radians can presumably be attributed to the increased feed forces (see Fig. 17), which resulted from the increased cutting speed and thus led to a greater elastic deformation of the tools and longer engagement times. In cutting processes, the cutting force components initially increase with increasing cutting speeds before they only decrease with a further increase of the cutting speed. The increase is usually attributed to the formation of built-up edges, while a further increase of the cutting speed leads to a further increase of the process temperatures and thus a decrease in the strength of the material and a reduction in the cutting force components. Especially when machining AlMgSi0.5, the feed forces have increased significantly. The hypothesis of built-up edge formation as the reason for the increase in the feed force therefore fits well with the observed results, since this material has a strong tendency to form built-up edges.

In summary, it can be said that the selected percentual cutting time can also be transferred to processes with increased cutting speeds in the present case. Due to increased feed forces at increased cutting speeds, a slight increase in the chip radians could be observed. However, it can be assumed that a further increase in the cutting speed will result in a decrease of the cutting force components. At this point it should be noted, that the chip removal quality can be affected by the effectively shorter interrupted cutting times, if the spindle speed is further increased. This applies especially for materials with a tendency for adhesions. In this case, the recommended amplitude is an appropriate starting point for a careful increase of the value. Using high cutting speeds in combination with high cutting forces can lead to torsional vibrations and chatter marks.

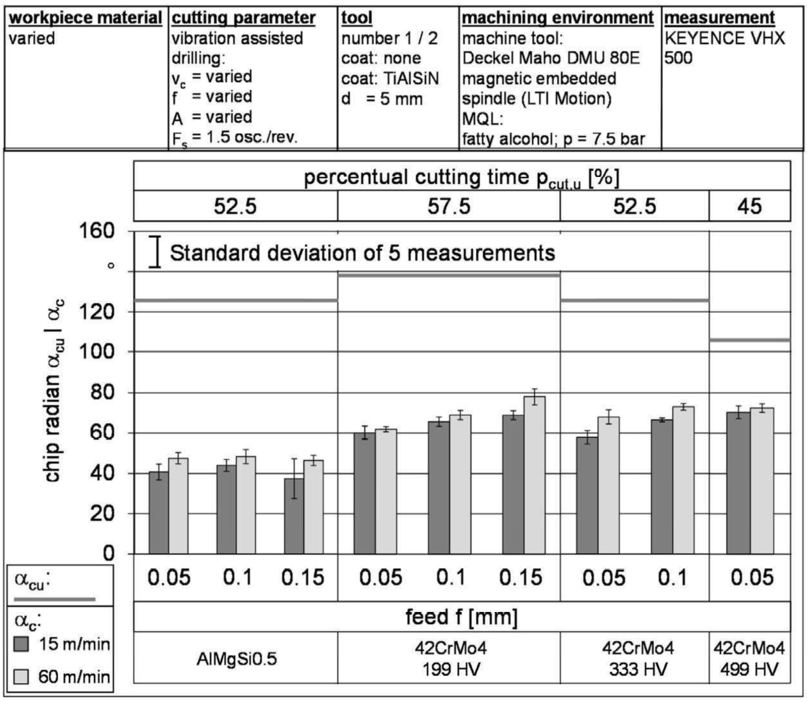

Fig. 16. Comparison of the uncut chip radians and chip radians, resulting from drilling processes at different cutting speeds.

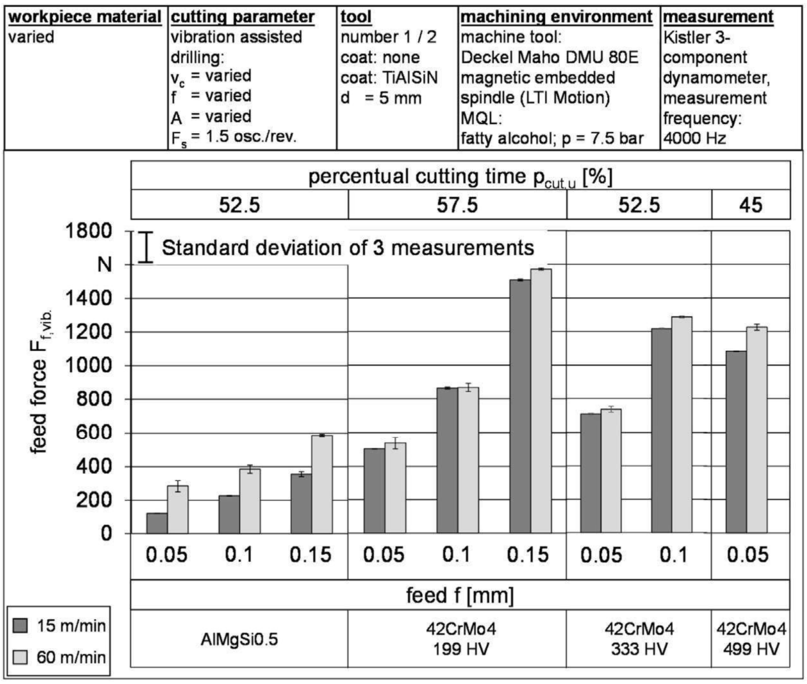

Fig. 17. Comparison of the feed forces, resulting from drilling processes at different cutting speeds.

Summary and conclusion

In summary, the workpiece material properties which are mainly responsible for the specific differences in the resulting chip geometry and chip removal quality could be identified and direct parameter recommendations regarding the optimal amplitude for LFVAD processes in different materials could be determined. High (temperature) strength values are leading to a lower chip compression. Therefore the oscillation amplitude has to be increased. Workpiece materials with an adhesion tendency require higher oscillation amplitudes to ensure interrupted cutting times, high enough to lift-off the chips from the cutting edges. At a combination of high (temperature) strength and a high adhesion tendency, very low percentual cutting times are required (see Ti6Al4V). The ductility or toughness of the workpiece material seems to be less relevant, due to the interrupted cut in LFVAD, leading to an enforced chip breakage. In strongly divergent applications, the determined amplitude values possibly have to be adjusted to boundary conditions like the tool geometry (chip space, internal coolant holes, cutting edge radius), the stiffness of the workpiece clamping and the MQL pressure/flow rate, but the key findings can be transferred to a wide range of workpiece materials and applications of LFVAD. Furthermore, the presented investigations have been shown, that the findings can be transferred to varying cutting speeds as well. In this context has to be mentioned, that variations of the cutting speed can affect the feed forces, the elasto-plastic material behavior and the interrupted cutting times, resulting in slightly modified chip sizes. Additionally, the chip removal quality can be affected by the effectively shorter interrupted cutting times, when drilling at further increased cutting speeds. Especially when drilling aluminium alloys with a strong tendency to adhesions, an upper limit of the possible spindle speed/cutting speed will occur, which has to be determined in further investigations.

Conflicts of interest

The authors declare that they have no known competing financial interests or personal relationships that could have appeared to influence the work reported in this paper.

Acknowledgements

The authors would like to thank Gühring KG for the provision of drilling tools and KEBA Industrial Automation Germany GmbH (formerly LTI Motion GmbH) for the professional technical advice and support in the work with the magnetically embedded spindle. Additionally, the authors would like to thank the German Federation of Industrial Research Associations (AiF) for funding the research work within the project 19473 N/1.

References

[1] Heisel, U., Wallaschek, J., Eisseler, R., Potthast, C., 2008, Ultrasonic Deep Hole Drilling in Electrolytic Copper ECu 57. CIRP Annals Manufacturing Technology, 57/1: 53–56.
[2] Bleicher, F., Wiesinger, G., Kumpf, C., Finkeldei, D., Baumann, C., Lechner, C., 2018, Vibration Assisted Drilling of CFRP/Metal Stacks at Low Frequencies and High Amplitudes. Production Engineering, 12:289–296.
[3] Biermann, D., Bleicher, F., Heisel, U., Klocke, F., Möhring, H.-C., Shih, A., 2018, Deep Hole Drilling. CIRP Annals Manufacturing Technology, 67/2: 673–694.
[4] Brinksmeier, E., Pecat, O., Rentsch, R., 2015, Quantitative Analysis of Chip Extraction in Drilling of Ti6Al4V. CIRP Annals Manufacturing Technology, 64/1: 93–96.
[5] Armendia, M., Garay, A., Villar, A., Davies, M.A., Arrazola, P.J., 2010, High Bandwidth Temperature Measurement in Interrupted Cutting of Difficult to Machine Materials. CIRP Annals Manufacturing Technology, 59/1: 97–100.
[6] Paulsen, T., Pecat, O., Brinksmeier, E., 2016, Influence of Different Machining Conditions on the Subsurface Properties of Drilled TiAl6V4. Procedia CIRP, 46:472–475.
[7] Abdelhafeez, A.M., Soo, S.L., Aspinwall, D.K., Dowson, A., Arnold, D., 2018, The Influence of Burr Formation and Feed Rate on the Fatigue Life of Drilled Titanium and Aluminium Alloys used in Aircraft Manufacture. CIRP Annals Manufacturing Technology, 67/1: 103–108.
[8] Pecat, O., Brinksmeier, E., 2014, Low Damage Drilling of CFRP/Titanium Compound Materials for Fastening. Procedia CIRP, 13:1–7.
[9] Hussein, R., Sadek, A., Elbestawi, M.A., Attia, M.H., 2018, Low-Frequency Vibration-Assisted Drilling of Hybrid CFRP/Ti6Al4V Stacked Material. International Journal of Advanced Manufacturing Technology, 98:2801–2817.
[10] Pecat, O., 2018, Vibrationsunterstütztes Bohren von Werkstoffverbunden aus CFK und Titan, PhD thesis. IWT Bremen.
[11] Yang, H., Ding, W., Chen, Y., Laporte, S., Jiuhua, X., Fu, Y., 2019, Drilling Force Model for Forced Low Frequency Vibration Assisted Drilling of Ti-6Al-4V Titanium Alloy. International Journal of Machine Tools and Manufacture, 146103438.
[12] Pecat, O., Paulsen, T., Katthöfer, P., Brinksmeier, E., Fangmann, S., 2016, Vibration Assisted Drilling of Aerospace Materials. SAE Technical Paper, 01:2136.

[13] Ikuta, A., Shinozaki, K., Masuda, H., Yamane, Y., Kuroki, H., Fukaya, Y., 2002, Consideration of the Adhesion Mechanism of Ti Alloys Using a Cemented Carbide Tool During the Cutting Process. Journal of Materials Processing Technology, 127:251–255.

[14] Nouari, M., List, G., Girot, F., Géhin, D., 2005, Effect of Machining Parameters and Coating on Wear Mechanisms in Dry Drilling of Aluminium Alloys. International Journal of Machine Tools and Manufacture, 45:1436–1442.